

Enabling AI Quality Control via Feature Hierarchical Edge Inference

Jinhyuk Choi*, Seong-Lyun Kim*, Seung-Woo Ko[§]

*School of EEE, Yonsei University, Seoul, Korea, email: {jh.choi, slkim}@ramo.yonsei.ac.kr

[§]Dept. of Smart Mobility Eng., Inha University, Incheon, Korea, email: swko@inha.ac.kr

Abstract—With the rise of edge computing, various AI services are expected to be available at a mobile side through the inference based on *deep neural network* (DNN) operated at the network edge, called *edge inference* (EI). On the other hand, the resulting AI quality (e.g., mean average precision in objective detection) has been regarded as a given factor, and AI quality control has yet to be explored despite its importance in addressing the diverse demands of different users. This work aims at tackling the issue by proposing a *feature hierarchical EI* (FHEI), comprising feature network and inference network deployed at an edge server and corresponding mobile, respectively. Specifically, feature network is designed based on feature hierarchy, a one-directional feature dependency with a different scale. A higher scale feature requires more computation and communication loads while it provides a better AI quality. The tradeoff enables FHEI to control AI quality gradually w.r.t. communication and computation loads, leading to deriving a near-to-optimal solution to maximize multi-user AI quality under the constraints of uplink & downlink transmissions and edge server and mobile computation capabilities. It is verified by extensive simulations that the proposed joint communication-and-computation control on FHEI architecture always outperforms several benchmarks by differentiating each user's AI quality depending on the communication and computation conditions.

I. INTRODUCTION

Due to the rapid advancement of *artificial intelligence* (AI), a wide range of mobile services has been built on an AI framework, e.g., Tensorflow and Torch, to offer accurate and reliable results by inferring the most likely outcomes using a well-trained *deep neural network* (DNN). Edge computing-based inference, shortly *edge inference* (EI), is expected to be its crucial enabler such that an edge server nearby runs the DNN to execute mobiles' inference tasks [1].

In an early stage of EI research, an AI model is assumed to be indivisible and installed at either a mobile or an edge server with communication efficient offloading techniques (see e.g., [2] and [3]). With the recent rise of split learning [4], it is possible to divide the entire AI model into multiple sub-models, called *model partitioning* (MP). With MP, mobiles and an edge server can cooperate to perform EI, thereby reducing the computation load and computation latency. For example, in [5], mobiles are in charge of extracting and encoding task-specific features from raw data based on the well-known information bottleneck principle, while the edge server proceeds the remaining EI by receiving the encoded features. Prompted by BranchyNet proposed in [6], the concept of early exit is introduced in [7] that multiple branches in the DNN return different features used as inputs to the corresponding EI processes. The time required to reach each branch is different,

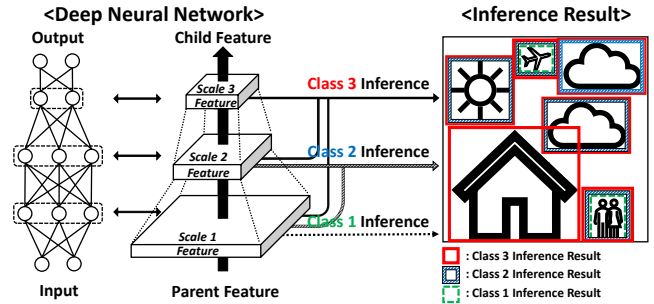


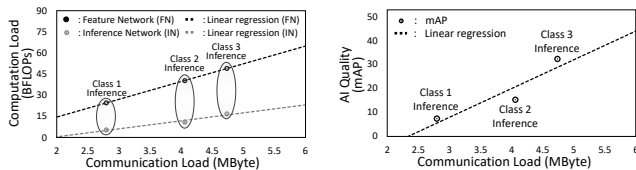
Fig. 1. Graphical representation of feature hierarchy of a DNN-based AI model. A class- k inference is defined as the inference using the features of scales 1 to k as inputs, achieving a more qualified result than a lower class one.

allowing the system to determine one of them as an exit branch depending on the computation latency requirement.

As aforementioned, most prior works on EI focuses on addressing the load balancing and latency issues, whereas the quality of AI has not been considered yet due to the following two reasons. First, the concerned DNN architecture returns an output with a single quality (e.g., [5]). Second, the result through a heavier computation does not guarantee a better quality (e.g., [7]), hindering an elastic control of AI quality on the concerned DNN architecture.

This work attempts to tackle the issue of controlling AI quality by exploiting feature hierarchy explained as follows. As shown in Fig. 1, each layer's activation pattern during a DNN operation corresponds to a feature vector extracted from the input data. It is well-known that the feature from a deeper layer can represent a larger scale of input data. Then, we define a feature of scale k as the features extracted from the k -th layer. Due to a forward propagation process, the features of scales $(k - 1)$ and k have a hierarchical relation, transforming the former into the latter but not vice versa. The *feature pyramid network* (FPN) proposed in [8] is a representative DNN architecture designed based on feature hierarchy, showing that when features of different scales are simultaneously used as inputs for an inference task, the resultant output has a better quality, e.g., many targets with different scales are well captured for object detection. On the other hand, extracting different scales of features requires a heavier computation load.

Inspired by the above trade-off, we propose a *feature-hierarchical EI* (FHEI), which enables us to gradually control each mobile's AI quality. Specifically, we divide a feature hierarchy-based DNN into *feature network* (FN) and *inference*



(a) Computation load vs. Communication load (b) AI quality vs. Communication load

Fig. 2. The relation among computation load, AI quality, and communication loads of feature hierarchy-based DNN with 3 classes of inferences.

network (IN). Due to the heavy computation loads to extract multi-scale features, FN is installed at the edge server, while IN is located at each mobile to facilitate a user-customized service. The edge server adjusts the degree of feature scale depending on the user’s service quality demands under the constraints of its computation capability. Besides, FHEI requires not only uplink transmission to offload mobiles’ local data to the edge server but also downlink transmission to return the extracted features to the corresponding mobiles. As a result, a joint radio-and-computation resource optimization is required to maximize sum AI quality, verified to achieve superior performance to several benchmarks.

II. FEASIBILITY STUDY ON AI QUALITY CONTROL

This section studies the feasibility of AI quality control via the experiments explained below, leading to establishing the relation among multiple metrics with interesting insights.

A. Experiment Setting

We use the YOLO v3 for an object detection task, extracting multi-scale features based on FPN [8]¹. The concerned YOLO model is published in [11], which is trained using the 2017 *Common Object in COntext* (COCO) dataset comprising 118K image samples with 80 labels. The input size of model is 416×416 . For testing, we randomly select 500 samples among 5K validation samples in [12]. The number of layers in the YOLO model is 106, divided into FN from layers 1 to 75 and IN from layers 76 to 106. The number of feature scales is 3, providing 3 classes of inference services, namely, a class- k inference using features of scales from 1 to k , where $k \in \{1, 2, 3\}$.

B. Performance Metrics

We measure three performance metrics, each of which the definition and evaluation methods are explained below.

1) *Communication Load*: Based on the concerned Yolo v3 settings, the layer indices corresponding to 3 scales of features are $\mathbf{f} = [37, 62, 75]$. The resultant computation load of class- k inference is computed by summing up the output data sizes of layers from $\mathbf{f}(1)$ to $\mathbf{f}(k)$.

¹Various DNN structures built on feature hierarchy exist in the literature, such as U-Net [9] and a Laplacian pyramid [10]. The experiments in the section are applicable to them, remaining as future work due to the page limit.

2) *Computation Load*: Denote ℓ_j the computation load (in FLOPs) for layer j , which can be computed as

$$\ell_j = k_j^2 m_j^2 h_{j-1} h_j, \quad (1)$$

where k_j , m_j , and h_j represents the j -th convolution layer’s filter size, output size, and channel number, respectively. The resultant computation loads of class- k inference $L(k)$ is

$$L(k) = \sum_{j=1}^{\mathbf{f}(k)} \ell_j + \sum_{j=\mathbf{i}(k)}^{\mathbf{i}(k)+6} \ell_j, \quad (2)$$

where the first and second terms represent the computation loads of FN and IN, respectively. Here, each IN comprises 7 consecutive layers whose starting index is $\mathbf{i} = [76, 88, 100]$.

3) *AI Quality*: AI quality can be represented by the precision defined as the probability of detecting objectives correctly. *Mean average precision* (mAP) is the expected precision averaged over objects annotated by different labels. Among several mAP computation methods in the literature, we adopt the technique in [13], which is widely used in many object detection applications.

C. Observations and Insights

Fig. 2 represents the relation among communication load (in MBytes), computation load (in BFLOPs), and AI quality (in mAP) when different classes of inferences are considered. Several interesting observations are made as follows, motivating us to design our system model and formulate the problem introduced in the sequel.

1) *Effect of a Different Class Inference*: A higher class inference results in heavier communication & computation loads and better AI quality.

2) *Linearity w.r.t. Communication Load*: Through a linear regression, computation load and AI quality tend to be linearly increasing as a communication load becomes heavier due to a higher class of inference. In other words, a communication load can be interpreted as a controllable variable to adjust both computation load and AI quality.

3) *Feature Network’s Computation Load Bias*: As shown in Fig. 2(a), FN’s computation load is positively biased when the corresponding communication load is the minimum, i.e. 2 MBytes, which is a baseline computation load to initiate FN. On the other hand, IN’s computation load is unbiased.

III. FEATURE HIERARCHICAL EDGE INFERENCE: ARCHITECTURE AND PROBLEM FORMULATION

Prompted by Sec. II, we propose FHEI to control multiple mobiles’ AI qualities. To this end, we firstly introduce the system architecture of FHEI. Next, several key performance metrics are explained. Last, the optimization problem maximizing the sum of each mobile’s AI quality is formulated.

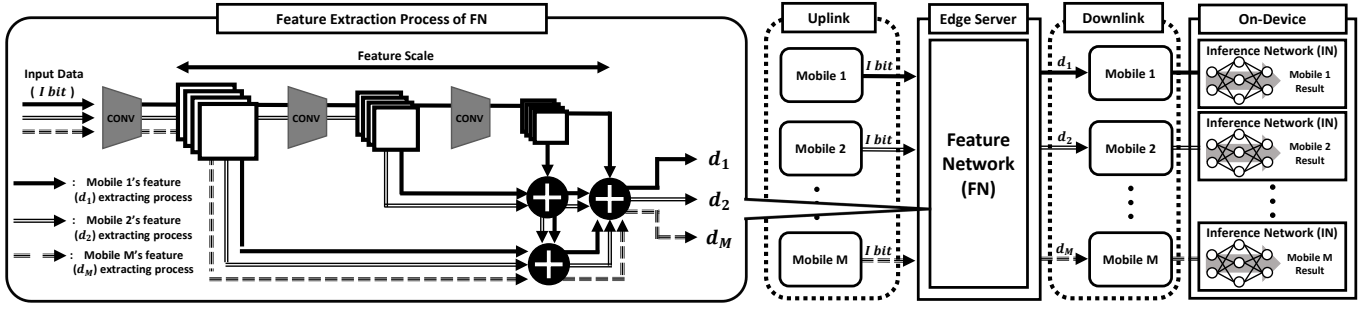


Fig. 3. Schematic architecture of FHEI, comprising a single edge server and multiple mobiles. The edge server operates FN to extract different scales of features based on the principle of feature hierarchy, and each mobile inputs the extracted feature into the corresponding IN for its corresponding inference service.

A. Architecture

Consider a wireless network comprising M mobiles, denoted by $\mathbb{M} = \{1, \dots, M\}$, and an AP linked to an edge server (see Fig. 3). Each mobile attempts to run a DNN-based inference program by the aid of the edge server. To this end, the proposed FHEI splits the computation loads between the edge server and the mobiles, as explained below.

1) *Edge Inference*: Consider a DNN-based inference program, denoted by \mathcal{P}_m , which can be divided into FN $\{\mathcal{F}_m\}$ and IN $\{\mathcal{I}_m\}$. The mobile m 's raw data is fixed to certain I Bytes². The relation among \mathcal{P}_m , \mathcal{F}_m , and \mathcal{I}_m is given as

$$\mathcal{P}_m(\mathbf{a}_m) = \mathcal{I}_m(\mathcal{F}_m(\mathbf{a}_m)) = \mathcal{I}_m(\mathbf{b}_m), \quad (3)$$

where \mathbf{a}_m and \mathbf{b}_m are vectors representing input and feature for mobile m 's program, respectively.

For an effective FN operation, a feature hierarchy-based unified FN can be installed at the edge server, denoted by \mathcal{F} , which can cover all mobiles' FNs $\{\mathcal{F}_m\}$, i.e., $\mathcal{F}_m \subset \mathcal{F}$ for all $m \in \mathbb{M}$. Specifically, the unified FN \mathcal{F} follows a feature hierarchy architecture, divided into two parts. The first part includes base layers to initiate the feature extraction. The second one includes hierarchical feature extraction layers such that the scale- k feature with the size of $d^{(k)}$ is extracted from the corresponding layer. The unified FN $\{\mathcal{F}\}$ can operate as mobile m 's FN by extracting the scales of features from 1 to $k^*(m)$ defined as

$$k^*(m) = \inf_k \left\{ d_m \leq \sum_{\ell=1}^k d^{(\ell)} \right\}, \quad (4)$$

where d_m represents the size of mobile m 's extracted feature.

Following the observations in Sec. II-C3 and computation model in [2], the resultant computation load for mobile m 's feature extraction (in FLOPs) is given as

$$L_m^{(\text{FN})} = L_0 + c_1 \sum_{\ell=1}^{k^*(m)} d^{(\ell)} \geq L_0 + c_1 d_m, \quad (5)$$

where L_0 (FLOPs) is base layers' computation load and c_1 (FLOPs/Byte) is constant depending on the concerned FN.

²Every mobile's raw data size is assumed to be constant, since it is resized depending on a DNN's predefined input format.

For tractability, we assume that possible scales of feature are well fragmented enough to find $k^*(m)$ satisfying $d_m = \sum_{\ell=1}^{k^*(m)} d^{(\ell)}$ and $L_m^{(\text{FN})} = L_0 + c_1 d_m$, allowing us to use d_m as a control variable of the optimization introduced in the sequel.

On the other hand, IN $\{\mathcal{I}_m\}$ remains at mobile m 's side to facilitate user-customized services. As observed before, the computation load of mobile m 's IN $\{\mathcal{I}_m\}$ is unbiased and linearly increasing of the data size d_m , given as

$$L_m^{(\text{IN})} = c_2 d_m, \quad (6)$$

where c_2 (FLOPs/Byte) is constant.

2) *Wireless Communication*: The above computation architecture involves both uplink and downlink transmissions by splitting DNN into FN and IN. To this end, frequency bands for uplink and downlink are exclusively used with the fixed bandwidths of W_U and W_D , respectively.

We consider *time division multiple access* (TDMA) to allows multiple mobiles to access the medium simultaneously. Mobile m 's uplink and downlink channel gains are denoted by $g_{m,U}$ and $g_{m,D}$, which are assumed to be stationary within the concerned duration of EI. Following Shannon capacity, the uplink and downlink maximum data rates (in bps) become $U_m = W_U \log_2 \left(1 + \frac{g_{m,U} P_U}{N_0 W_U} \right)$ and $D_m = W_D \log_2 \left(1 + \frac{g_{m,D} P_D}{N_0 W_D} \right)$, where P_U and P_D are transmit power of each mobile and AP, and N_0 is a noise spectral density (in Watts/Hz). We denote α_m and β_m the time portions assigned for mobile m 's uplink and downlink transmissions satisfying $\sum_{m \in \mathbb{M}} \alpha_m \leq 1$ and $\sum_{m \in \mathbb{M}} \beta_m \leq 1$. The resultant achievable rates (in bps) are thus given as

$$\Lambda_m = \alpha_m U_m, \quad \Gamma_m = \beta_m D_m. \quad (7)$$

B. Key Performance Indicators

1) *End-to-End Latency*: An E2E latency (in sec), denoted by T_m , is defined as the duration required to return a mobile m 's inference result, which is expressed as the sum of communication and computation latencies, namely,

$$T_m = T_m^{(\text{comm})} + T_m^{(\text{comp})}. \quad (8)$$

First, communication latency, say $T_m^{(\text{comm})}$, consists of uplink duration to offload mobile m 's raw data to the edge server and downlink duration to download the extracted features from the

edge server. Given the data sizes of raw data and extracted features, say I and d_m , the communication delay is given as

$$T_m^{(\text{comm})} = \frac{I}{\Lambda_m} + \frac{d_m}{\Gamma_m}, \quad (9)$$

where Λ_m and Γ_m are mobile m 's uplink and downlink achievable rates specified in (7). Second, computation latency, say $T_m^{(\text{comp})}$, consists of an edge server's computation duration for the feature extraction and mobile m 's computation duration for the inference of the final result. Assuming that the edge server grants its partial computation resource with the speed of f_m (FLOPs/sec) for mobile m , the former is given as $\frac{L_m^{(\text{FN})}}{f_m}$. On the other hand, mobile m computation resource with the speed of q_m (FLOPs/sec) can be entirely used to infer its result. The latter then becomes $\frac{L_m^{(\text{IN})}}{q_m}$. The overall computation latency is

$$T_m^{(\text{comp})} = \frac{L_m^{(\text{FN})}}{f_m} + \frac{L_m^{(\text{IN})}}{q_m}. \quad (10)$$

By plugging (9) and (10) into (8), E2E latency for mobile m is given as

$$T_m = \frac{I}{\Lambda_m} + \frac{d_m}{\Gamma_m} + \frac{L_m^{(\text{FN})}}{f_m} + \frac{L_m^{(\text{IN})}}{q_m}. \quad (11)$$

2) *Mobile Energy Consumption*: Each mobile consumes its energy when communicating with the edge server and computing the final inference result, namely,

$$E_m = E_m^{(\text{comm})} + E_m^{(\text{comp})}. \quad (12)$$

First, communication energy consumption, say $E_m^{(\text{comm})}$, consists of two parts. The first part represents the energy required to transmit mobile m 's raw data, which is the product of the transmit power P_U and offloading duration $\frac{I}{\Lambda_m}$. On the other hand, the latter represents the energy required to receive the extracted features from the edge server, which is the product of the receive power σ_m and receiving duration $\frac{d_m}{\Gamma_m}$. We regard σ_m as constant σ without loss of generality. The overall communication energy consumption is then given as

$$E_m^{(\text{comm})} = P_U \frac{I}{\Lambda_m} + \sigma \frac{d_m}{\Gamma_m}. \quad (13)$$

Second, following the model in [14], computation energy consumption, say $E_m^{(\text{comp})}$, is proportional to the product between the square of computation speed q_m and computation load $L_m^{(\text{IN})}$, namely,

$$E_m^{(\text{comp})} = \psi q_m^2 L_m^{(\text{IN})}, \quad (14)$$

where ψ is the coefficient of computing-energy efficiency.

By plugging (13) and (14) into (12), the overall energy consumption of mobile m is

$$E_m = P_U \frac{I}{\Lambda_m} + \sigma \frac{d_m}{\Gamma_m} + \psi (q_m)^2 L_m^{(\text{IN})}. \quad (15)$$

C. Problem Formulation

This subsection formulates the problem of maximizing the sum of AI qualities. First, as discussed in Sec. II, we define an AI quality as a linear function of a mobile's communication load equivalent to the corresponding feature size d , namely,

$$\mathcal{U}(d) = \delta_s d, \quad (16)$$

where δ_s is constant depending on the concerned DNN AI model. Next, we introduce the following optimization problem maximizing the sum of each mobile's AI quality:

$$\begin{aligned} & \max_{\mathbf{d}, \boldsymbol{\alpha}, \boldsymbol{\beta}, \mathbf{f}, \mathbf{q}} \sum_{m \in \mathbb{M}} \mathcal{U}(d_m) & (P1) \\ \text{s.t. } & d_{\min} \leq \mathbf{d} \leq d_{\max}, & (\text{Feature Size Constraints}) \\ & \boldsymbol{\alpha}^T \mathbf{1} \leq 1, \quad \boldsymbol{\beta}^T \mathbf{1} \leq 1, & (\text{Radio Resource constraints}) \\ & \mathbf{f}^T \mathbf{1} \leq F, \quad \mathbf{q} \preceq \bar{\mathbf{q}}, & (\text{Computation resource constraints}) \\ & \frac{1}{M} \sum_{m \in \mathbb{M}} E_m \leq \bar{E}, & (\text{Average E2E Energy constraint}) \\ & \frac{1}{M} \sum_{m \in \mathbb{M}} T_m \leq \bar{T}, & (\text{Average E2E Latency constraint}) \end{aligned}$$

where $\mathbf{1}$ is a column vector whose all components are 1. Each constraint in P1 is explained with relevant definitions.

1) *Feature Sizes*: Denote $\mathbf{d} = [d_1, \dots, d_M]^T$ a vector whose elements are mobiles' feature sizes, each of which is between d_{\min} and d_{\max} under the constraints below.

2) *Radio Resources*: Denote $\boldsymbol{\alpha} = [\alpha_1, \dots, \alpha_M]^T$ and $\boldsymbol{\beta} = [\beta_1, \dots, \beta_M]^T$ vectors representing mobiles' uplink and downlink time portions, respectively, which are exclusively used for each mobile and limit their sums less than 1.

3) *Computation Resources*: Denote $\mathbf{f} = [f_1, \dots, f_M]^T$ a vector whose m -th component, say f_m , represents the edge server's computation resource allocated to mobile m (in FLOPs/sec). The sum of every component cannot exceed the maximum capability defined as F . Similarly, $\mathbf{q} = [q_1, \dots, q_M]^T$ is defined as a vector whose m -th component, say q_m , represents mobile m 's computation resource (in FLOPs/sec), less than Q_m , where $\bar{\mathbf{q}} = [Q_1, \dots, Q_M]^T$.

4) *E2E Latency and Energy Consumption Constraints*: The E2E latency and energy consumption, specified in (11) and (15) respectively, should be on average less than their requirements of \bar{T} (in sec) and \bar{E} (in Joule).

IV. AI QUALITY OPTIMIZATION OF FEATURE HIERARCHICAL EDGE INFERENCE

A. Problem Reformulation and Overview

This section aim at solving Problem P1. The main difficulty lies on the non-convexity of P1 since the average E2E latency and energy constraints include the terms of multiplying the feature size of d_m with other variables representing radio and computation resources. It can be overcome by decomposing P1 into the following two sub-problems.

$$\begin{aligned} \mathcal{L} = & \frac{1}{M} \sum_{m \in \mathbb{M}} \left(P_U \frac{I}{\Lambda_m} + \sigma \frac{d_m}{\Gamma_m} + \psi(q_m)^2 c_2 d_m \right) + \lambda \left(\frac{1}{M} \sum_{m \in \mathbb{M}} \left(\frac{I}{\Lambda_m} + \frac{d_m}{\Gamma_m} + \frac{L_0 + c_1 d_m}{f_m} + \frac{c_2 d_m}{q_m} \right) - \bar{T} \right) \\ & + \mu \left(\sum_{m \in \mathbb{M}} \alpha_m - 1 \right) + \gamma \left(\sum_{m \in \mathbb{M}} \beta_m - 1 \right) + \theta \left(\sum_{m \in \mathbb{M}} f_m - F \right) + \sum_{m \in \mathbb{M}} \zeta_m (q_m - Q_m), \end{aligned} \quad (17)$$

1) *Joint Radio-and-Computation Optimization*: The first sub-problem focuses on optimizing radio and computation resources, say α , β , f , and q , assuming that the feature size d is given. Specifically, the objective is to minimize the energy consumption conditioned on d by optimizing the above variables under the constraints of radio and computation resources and the average E2E latency, as stated below.

$$\begin{aligned} \min_{\alpha, \beta, f, q} & \frac{1}{M} \sum_{m \in \mathbb{M}} E_m \\ \text{s.t.} & \frac{1}{M} \sum_{m \in \mathbb{M}} T_m \leq \bar{T}, \\ & \alpha^T \mathbf{1} \leq 1, \quad \beta^T \mathbf{1} \leq 1, \quad f^T \mathbf{1} \leq F, \quad q \preceq \bar{q}. \end{aligned} \quad (\text{P2})$$

2) *AI Quality Optimization*: Given the variables optimized in P2, the second sub-problem is to maximize the sum of AI qualities under the constraint of the average energy consumption as follows.

$$\begin{aligned} \max_{\mathbf{d}} & \sum_{m \in \mathbb{M}} \mathcal{U}(d_m) \\ \text{s.t.} & d_{\min} \leq \mathbf{d} \leq d_{\max}, \quad \frac{1}{M} \sum_{m \in \mathbb{M}} E_m \leq \bar{E}. \end{aligned} \quad (\text{P3})$$

Due to the above decomposition, both P2 and P3 are convex problems, enabling us to derive their closed form solutions using the optimization theory, introduced in Sec. IV-B and Sec. IV-C, respectively. Next, solving P2 and P3 in an iterative manner leads to reach a near-to-optimal solution, whose convergence is explained in Sec. IV-D.

B. Optimal Radio-and-Computation Resource Allocation

This section targets to solve P2. Define a Lagrangian function \mathcal{L} as (17) shown in the top of the page, where λ , μ , γ , θ and $\zeta = \{\zeta_1, \dots, \zeta_N\}$ denotes Lagrange multipliers associated with the average E2E latency, uplink and downlink bandwidth constraints, edge server and device computation resource constraints, respectively. First, using *Karush Kuhn Tucker* (KKT) conditions, the optimal structures of α , β , and f are derived in terms of λ , μ , γ , θ , given as

$$\begin{aligned} \alpha_m^* &= \sqrt{\frac{I(P_U + \lambda^*)}{\mu^* M U_m}}, \quad \beta_m^* = \sqrt{\frac{d_m(\sigma + \lambda^*)}{\gamma^* M D_m}}, \\ f_m^* &= \sqrt{\frac{\lambda^*(L_0 + c_1 d_m)}{M \theta^*}}, \end{aligned} \quad (18)$$

whose derivations are omitted due to the page limit. It is observed that μ^* , γ^* , and θ^* should be strictly positive for feasible α_m^* , β_m^* , and f_m^* , respectively. Due to the slackness

condition, the equality conditions of corresponding constraints should be satisfied. Plugging the above optimal structure into the equality condition leads to deriving the closed form solutions of α_m^* , β_m^* , and f_m^* , summarized below.

Proposition 1 (Optimal Uplink & Downlink Transmissions and Edge Computing). The optimal solutions of α_m^* , β_m^* , and f_m^* for Problem P2 are given as

$$\begin{aligned} \alpha_m^* &= \frac{\frac{1}{\sqrt{U_m}}}{\sum_{n \in \mathbb{M}} \frac{1}{\sqrt{U_n}}}, \quad \beta_m^* = \frac{\sqrt{\frac{d_m}{D_m}}}{\sum_{n \in \mathbb{M}} \sqrt{\frac{d_n}{D_n}}}, \\ f_m^* &= F \frac{\sqrt{L_0 + c_1 d_m}}{\sum_{n \in \mathbb{M}} \sqrt{L_0 + c_1 d_n}}, \end{aligned}$$

which is independent of mobiles' computation speed q .

The optimal solution in Proposition 1 gives the minimum time required for uplink & downlink transmissions and FN execution to assign more time for each mobile's local computing of IN. In other words, Problem P2 becomes infeasible if the resultant duration of Proposition 1, which is the minimum duration before local computing, exceeds the E2E threshold \bar{T} . The subsequent explanation assumes that the duration is less than \bar{T} .

Next, the KKT condition associated with q_m , say $\frac{\partial \mathcal{L}}{\partial q_m} = 0$, can be manipulated as

$$2\psi q_m c_2 d_m + \zeta_m - \lambda c_2 \frac{d_m}{q_m^2} = 0, \quad (19)$$

whose closed-form solution is given as

$$q_m^* = \begin{cases} \sqrt[3]{\frac{\lambda^*}{2\psi}} & \text{if } \zeta_m = 0, \\ Q_m & \text{if } \zeta_m > 0, \end{cases} \quad (20)$$

where mobile m 's maximum computation speed Q_m is specified in Sec. III-C3. Noting that the optimal Lagrange multiplier λ^* should be strictly positive for non-negative f_m^* , the corresponding constraint, say the average E2E delay condition, satisfies the equality due to the slackness condition, namely,

$$\sum_{m \in \mathbb{M}} \frac{c_2 d_m}{q_m^*} = M \bar{T} - \sum_{m \in \mathbb{M}} \left(\frac{I}{\Lambda_m^*} + \frac{d_m}{\Gamma_m^*} + \frac{L_0 + c_1 d_m}{f_m^*} \right). \quad (21)$$

Plugging (20) into (21) leads to the following proposition.

Proposition 2 (Optimal Local Computing). The optimal solution of q_m^* for Problem P2 is

$$q_m^* = \min \left\{ \sqrt[3]{\frac{\lambda^*}{2\psi}}, Q_m \right\}, \quad (22)$$

where λ^* satisfies (21).

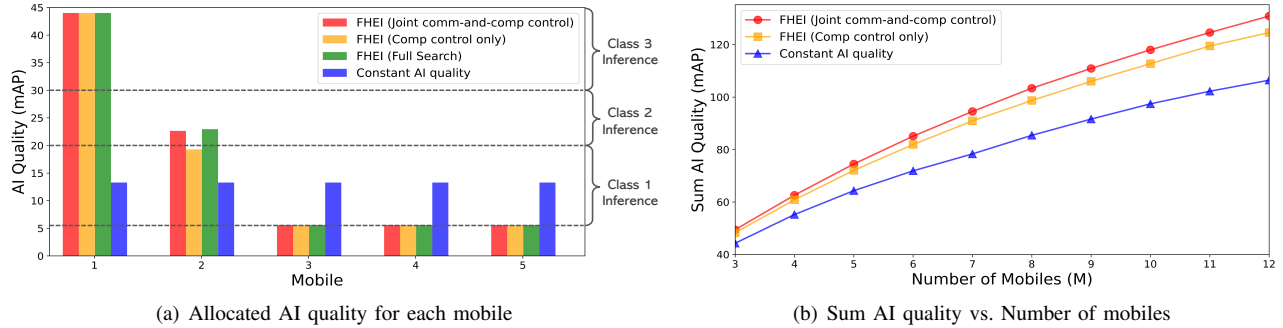


Fig. 4. The performance of FHEI (a) Individual AI quality for each mobiles. The uplink and downlink channel gains of each mobile are given as $[0.05, 1.32, 1.95, 4.63, 3.43]$ and $[5.17, 1.66, 1.51, 0.62, 1.14]$, respectively. (b) Average sum AI quality versus the number of mobiles. The uplink and downlink channel gains follow an independent gamma distribution with unit mean and scale factor of 3. Other parameters are specified in Table I.

C. Optimal AI Quality

Noting that Problem P3 is a linear optimization, we can solve it by a well-known greedy algorithm [15] whose detailed process is omitted due to the page limit.

D. Convergence

This section discusses the convergence to a near-to-optimal solution for P1 by solving Problems P2 and P3 attractively. As mentioned before, P2 is optimized based on P3's optimization result, leading to a monotone increasing of the sum of AI qualities until the optimized solution of P3 is feasible in P2. In other words, the iteration is stopped when P3's solution becomes infeasible in P2.

Through extensive numerical studies, one observes that the algorithm is sometimes terminated before reaching an optimal solution especially when the increase of the feature data size d is significant compared with the previous round. It is overcome by adding a constraint limiting the maximum increment per one round in P3, given as

$$\sum_{m \in \mathcal{M}} d_m \leq M \min\{d_{\min} \eta^{k-1}, d_{\max}\}, \quad (23)$$

where $\eta > 1$ is the increment ratio and k is the round number. Note that (23) is a linear constraint, and P3 with (23) is solvable using the same method specified in Sec. IV-C. We set $\eta = 1.01$, whose effectiveness is verified in the following section.

V. NUMERICAL RESULTS AND CONCLUDING REMARKS

This section represents simulation results to verify the effectiveness of FHEI on AI quality control. The concerned parameters are based on the experiment using YOLO v3 in Sec. II, summarized in Table I. We consider two benchmarks: constant AI quality and FHEI with computation resource optimization only. For the first benchmark, every mobile's AI quality is fixed but optimized under the same constraints as the proposed FHEI. For the second benchmark, uplink and downlink resources are allocated according to a channel inversion algorithm, while computation resources are optimized following the method in Sec. IV.

TABLE I
SIMULATION SETTINGS

Notation	Description	Value
M	# of mobiles	5
P_U	Uplink transmit power	0.1W
σ	Downlink receive power	0.01W
W_U	Uplink bandwidth	20 MHz
W_D	Downlink bandwidth	160 MHz
F	Edge server computation resource	20 TFLOPS
Q_m	Mobile m 's computation resource	1.5 ~ 4.5 GFLOPS
I	Data size of raw data	100 Kbytes
d_{\min}	Minimum feature size	2.8 Mbytes
d_{\max}	Maximum feature size	6 Mbytes
c_1	Coefficient of FN	12.59×10^3 FLOPs/Byte
c_2	Coefficient of IN	5.664×10^3 FLOPs/Byte
L_0	Constant computation load of FN	14.527 BFLOPs
\bar{E}	Average E2E energy constraint	5 J
\bar{T}	Average E2E latency constraint	15 sec
ψ	Energy efficiency coefficient	10^{-28} FLOPs ³ \times J/sec ²
δ_s	Coefficient of quality function	12 mAP/Mbyte

Fig. 4 compares FHEI with the above benchmarks. In Fig. 4(a), each mobile's optimized AI quality is represented under the given channel conditions specified in the caption. The dotted parallel lines show class inference boundaries when applying the YOLO v3. Several key observations are made. First, the proposed algorithm achieves a near-to-optimal performance. Second, compared with the first benchmark, FHEI can differentiate each user's AI quality depending on a downlink channel state, thereby increasing the entire AI quality. Third, the proposed joint communication-and-computation design outperforms the second benchmark, verifying the validity of the optimization in Sec. IV. Last, the gap between the two becomes significant as more mobiles exist (see Fig. 4(b)).

This work focuses on leveraging feature hierarchy to enable AI quality control on EI architecture. On the other hand, several other directions exist for future work, such as applying feature hierarchy to edge learning systems and subsequent resource optimizations.

REFERENCES

- [1] J. Shao and J. Zhang, "Communication-computation trade-off in resource-constrained edge inference," *IEEE Commun. Mag.*, vol. 58, no. 12, pp. 20–26, 2020.

- [2] Z. Lin, S. Bi, and Y.-J. A. Zhang, "Optimizing AI service placement and resource allocation in mobile edge intelligence systems," *IEEE Trans. Wireless Commun.*, vol. 20, no. 11, pp. 7257–7271, 2021.
- [3] Z. Liu, Z. Wu, C. Gan, L. Zhu, and S. Han, "Datamix: Efficient privacy-preserving edge-cloud inference," in *European Conference on Computer Vision (ECCV)*. Springer, 2020, pp. 578–595.
- [4] M. Chen, D. Gündüz, K. Huang, W. Saad, M. Bennis, A. V. Feljan, and H. V. Poor, "Distributed learning in wireless networks: Recent progress and future challenges," *IEEE J. Sel. Areas Commun.*, 2021.
- [5] J. Shao, Y. Mao, and J. Zhang, "Task-oriented communication for multi-device cooperative edge inference," *IEEE Trans. Wireless Commun.*, 2022.
- [6] S. Teerapittayanon, B. McDanel, and H.-T. Kung, "Branchynet: Fast inference via early exiting from deep neural networks," in *Proc. 23rd Int. Conf. Pattern Recognit. (ICPR)*. IEEE, 2016, pp. 2464–2469.
- [7] E. Li, L. Zeng, Z. Zhou, and X. Chen, "Edge AI: On-demand accelerating deep neural network inference via edge computing," *IEEE Trans. Wireless Commun.*, vol. 19, no. 1, pp. 447–457, 2019.
- [8] T.-Y. Lin, P. Dollár, R. Girshick, K. He, B. Hariharan, and S. Belongie, "Feature pyramid networks for object detection," in *Proc. IEEE Conf. Comput. Vis. Pattern Recognit. (CVPR)*, 2017, pp. 2117–2125.
- [9] O. Ronneberger, P. Fischer, and T. Brox, "U-net: Convolutional networks for biomedical image segmentation," in *Proc. Int. Conf. Medical Image Comput. Comput.-Assisted Intervention*. Springer, 2015, pp. 234–241.
- [10] G. Ghiasi and C. C. Fowlkes, "Laplacian pyramid reconstruction and refinement for semantic segmentation," in *Proc. Eur. Conf. Comput. Vis.* Springer, 2016, pp. 519–534.
- [11] J. Redmon, S. Divvala, R. Girshick, and A. Farhadi, "You only look once: Unified, real-time object detection," in *Proc. IEEE Conf. Comput. Vis. Pattern Recognit. (CVPR)*, Jun. 2016, pp. 779–788.
- [12] T.-Y. Lin, M. Maire, S. Belongie, J. Hays, P. Perona, D. Ramanan, P. Dollár, and C. L. Zitnick, "Microsoft coco: Common objects in context," in *Proc. 13th Eur. Conf. Comput. Vis.* Springer, 2014, pp. 740–755.
- [13] R. Padilla, S. L. Netto, and E. A. Da Silva, "A survey on performance metrics for object-detection algorithms," in *Proc Int. Conf. Syst., Signals Image Process.* IEEE, 2020, pp. 237–242.
- [14] Y. Wang, M. Sheng, X. Wang, L. Wang, and J. Li, "Mobile-edge computing: Partial computation offloading using dynamic voltage scaling," *IEEE Trans. Commun.*, vol. 64, no. 10, pp. 4268–4282, 2016.
- [15] J. Edmonds, "Matroids and the greedy algorithm," *Mathematical programming*, vol. 1, no. 1, pp. 127–136, 1971.